



HAL
open science

Electron hopping at the Si(111):B-root 3 surface: Insight from local impurity spectroscopy

Cédric Tournier-Colletta, Bertrand Kierren, Yannick Fagot-Révurat, Daniel
Malterre

► **To cite this version:**

Cédric Tournier-Colletta, Bertrand Kierren, Yannick Fagot-Révurat, Daniel Malterre. Electron hopping at the Si(111):B-root 3 surface: Insight from local impurity spectroscopy. *Physical Review B: Condensed Matter and Materials Physics (1998-2015)*, 2013, 87 (7), 10.1103/PhysRevB.87.075427 . hal-01273649

HAL Id: hal-01273649

<https://hal.science/hal-01273649>

Submitted on 25 May 2023

HAL is a multi-disciplinary open access archive for the deposit and dissemination of scientific research documents, whether they are published or not. The documents may come from teaching and research institutions in France or abroad, or from public or private research centers.

L'archive ouverte pluridisciplinaire **HAL**, est destinée au dépôt et à la diffusion de documents scientifiques de niveau recherche, publiés ou non, émanant des établissements d'enseignement et de recherche français ou étrangers, des laboratoires publics ou privés.

Electron hopping at the Si(111):B- $\sqrt{3}$ surface: Insight from local impurity spectroscopy

C. Tournier-Colletta,* B. Kierren, Y. Fagot-Revurat, and D. Malterre

Institut Jean Lamour, UMR 7198, Nancy-Université, Boîte Postale 239, F-54506 Vandœuvre-lès-Nancy, France

(Received 19 October 2012; revised manuscript received 18 December 2012; published 19 February 2013)

Boron vacancies at the Si(111):B- $\sqrt{3}$ surface are model systems in the comprehension of strongly correlated semiconductor surfaces. By using scanning tunneling spectroscopy, the origin of the single-vacancy electronic structure is addressed. It is shown to originate from the localization of a well-identified dangling-bond surface state with significant B character. The bivacancy defect, which is characterized by energy-split bonding and antibonding states, is interpreted within the textbook diatomic molecule picture. From the hopping parameter, we determine the bandwidth of the surface state from which the impurity state derives and evaluate the strength of many-body effects. Our analysis supports the realization of the Mott-Hubbard insulator state in half-filled dangling-bond surface states on $\sqrt{3}$ -reconstructed surfaces, as proposed recently for SiC(0001), Sn/Ge(111), and Sn/Si(111).

DOI: [10.1103/PhysRevB.87.075427](https://doi.org/10.1103/PhysRevB.87.075427)

PACS number(s): 73.20.At, 71.27.+a, 73.20.Hb, 71.55.Cn

I. INTRODUCTION

Dangling bonds at semiconductor surfaces have been attracting considerable interest in the context of strongly correlated systems. Because of their *sp* orbital nature, dangling bonds are characterized by a Hubbard repulsion energy $U \approx 1$ eV (Ref. 1) that seemingly makes them unsuitable to exhibit strong correlation physics, unlike *d* or *f* electron systems. However, surface-state bands deriving from such dangling bonds exhibit a small bandwidth $W \approx 0.1$ eV because of the reduced dimensionality. That feature is strengthened by surface reconstructions that tend to seclude the dangling bonds from each other. A typical example is found on $\sqrt{3}$ -reconstructed surfaces where dangling bonds are separated by almost 7 Å.² As a consequence, dangling-bond surface states potentially verify the $U \gg W$ condition to trigger the Mott-Hubbard metal-to-insulator transition.³ Prototypical examples are found at the pristine SiC(0001)- $\sqrt{3}$ surface⁴ and in Sn/Ge(111)- $\sqrt{3}$ and Sn/Si(111)- $\sqrt{3}$ surface alloys,⁵⁻⁷ where *ab initio* calculations fail to reproduce the insulating nature of these surfaces.

At the Si(111):B- $\sqrt{3}$ surface, the electronic properties of single boron vacancies have been studied recently by means of scanning tunneling microscopy/spectroscopy (STM/STS).⁸⁻¹⁰ Their characteristic spectroscopic signature is an unoccupied resonance appearing in the intrinsic gap.⁸ This resonance derives from *sp_z* states and therefore is very similar to the dangling bonds that form upon creating a silicon surface. By further using very high tunneling currents, Nguyen *et al.* reached a permanent regime in which the impurity becomes singly occupied.¹⁰ In that regime, they observed a new resonance at higher energy, attributed to the addition of a second electron and separated by $U \approx 1$ eV, that is typical of silicon dangling bonds.¹ Independently of correlation effects, the transport process has been shown to be of polaronic nature as a result of strong electron-vibration coupling.⁸

In this paper, we report a low-temperature STS study of the electronic hopping at the Si(111):B- $\sqrt{3}$ surface that completes the previously cited works on many-body aspects. To start with, we show that the in-gap resonance results from the localization at the impurity site of a well-identified dangling-bond surface state with significant boron contribution. The

second important result is the evidence of coupling between two neighboring boron vacancies. This so-called bivacancy defect shows a striking similarity to the textbook homonuclear, diatomic molecule case. Bonding and antibonding states are indeed observed, and their energy separation allows to determine the hopping parameter between impurity states ($|t| = 80$ meV). By combining these two independent results, we can estimate the bandwidth of the dangling-bond surface state ($W = 0.64$ eV). Finally, the strength of many-body interactions is addressed by comparing the surface-state bandwidth to available many-body parameters in the literature. The analysis supports the realization of a Mott insulator in the half-filled dangling-bond surface state on $\sqrt{3}$ -reconstructed surfaces, as proposed recently for SiC(0001),⁴ Sn/Ge(111),^{5,7} and Sn/Si(111).^{6,7}

II. EXPERIMENT

The experiments were carried out in an ultrahigh vacuum setup, using a commercial LT-Omicron scanning tunneling microscope operated at either 5 or 77 K. Spectroscopic acquisition is achieved with the lock-in technique, in the open feedback-loop mode. Typical modulation bias and frequency were 30 meV and 700 Hz, respectively. The typical junction set point parameters were $I = 0.5$ nA and $U = +2$ V (unoccupied states). In order to produce the $\sqrt{3}$ -reconstructed surface, we used highly boron-doped Si(111) wafers (degenerate *p*-type semiconductor, $\rho \approx 10^{-3}$ Ω cm). The sample is annealed by direct heating, starting with repeated flash annealings at 1400 K followed by an annealing of several hours at a lower temperature (1100 K). This procedure ensures bulk B impurities are segregated at the surface and substitute Si atoms at the *S₅* site, leading to the $\sqrt{3}$ surface reconstruction with one B atom per reconstructed unit cell.¹¹ Those B atoms in the sublayer act as acceptors that accommodate the dangling bond electrons provided by Si adatoms, resulting in a passivated surface.

III. RESULTS

Figure 1 shows a constant-current STM image of an almost-defect-free surface ($U = +2$ V, $I = 0.3$ nA). Low-height

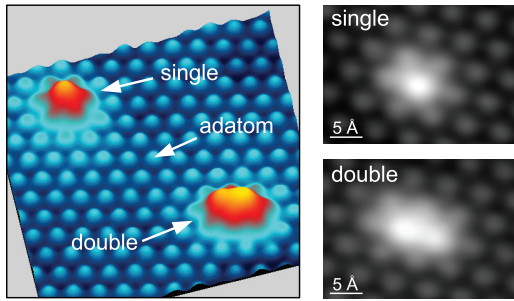


FIG. 1. (Color online) Atomically resolved STM image of the Si(111):B- $\sqrt{3}$ surface ($U = +2$ V, $I = 0.3$ nA). Besides passivated adatoms, we observe two kinds of defects associated with B vacancies in the sublayer: a single defect and a double defect, with the latter corresponding to two adjacent B vacancies.

protrusions (blue) correspond to passivated Si adatoms that are arranged in a $\sqrt{3}$ hexagonal array with 6.65-Å atomic spacing. In addition, two distinct bright features are observed. The first one (labeled single) is characterized by a single bright spot centered at an adatom position and surrounded by neighbors of higher apparent height than the passivated sites, giving this peculiar flower-like shape to the defect. This is attributed to a B vacancy in the sublayer. The strong contrast observed in the topographic image is a spectroscopic effect resulting from an unoccupied impurity state in the intrinsic gap that strongly contributes to the tunneling current.⁸ The second bright feature (labeled double) consists of two adjacent defects of the first kind. This so-called bivacancy is statistically difficult to detect on well-prepared surfaces. Although not shown here, a drastic reduction of the segregation time yields more of these defects and even more complex multiple vacancies.

In the context of strongly correlated surfaces, the electronic structure of Si(111):B- $\sqrt{3}$ provides interesting insight as it is a model system involving dangling-bond surface states. In Fig. 2(a), we present dI/dV maps recorded on the passivated surface at 5 K. At low energy [(i), 1.30 eV], the density of states (DOS) is centered on Si adatoms (labeled ad). By increasing the energy, the DOS first becomes structureless [(ii), 1.55 V] before showing a honeycomb pattern with a minimum at the adatom sites and a maximum over second-layer Si₂ atoms [(iii), 1.80 eV]. This dramatic change, visualized as a contrast inversion, is the indication that different electronic states are

probed at low and high energies. Alternatively, the point can be evidenced with energy-dependent dI/dV spectra [Fig. 2(b)]. On the adatom site (solid blue line), the local DOS shows an onset at 1.05 eV and a pronounced maximum at 1.80 eV. The spectrum recorded on the second-layer site (dashed red line) exhibits a similar energy dependence but shows a clear transfer of spectral weight from high to low energies (see inset). Therefore, low-energy (high-energy) electronic states show an enhanced density on ad (Si₂) sites. As expected, at the crossing point of the two spectra, the corresponding dI/dV map (ii) shows no contrast.

The origin of these electronic states is addressed by comparing the STS measurements to the available DFT calculations [Ref. 11; Fig. 2(b), right]. Along the $\bar{\Gamma}\bar{K}$ surface direction, the electronic structure exhibits two surface states, labeled SS₁ and SS₂, that overlap with the bulk conduction states (shaded gray area). The calculated band structure has been rigidly shifted in order to match the Fermi level with the top of the valence band, as expected in a degenerate p -type semiconductor. At the $\bar{\Gamma}$ point, the onset and the pronounced maximum of the experimental DOS coincide remarkably with SS₁ and SS₂, respectively. In the vicinity of $\bar{\Gamma}$, SS₂ has an almost flat dispersion that yields a peaked DOS as observed experimentally. In contrast, SS₁ disperses strongly, resulting in a spread DOS.

The analysis at $\bar{\Gamma}$ only is not sufficient since STS is a k -integrating technique, whose finite range of integration depends on the tip properties.¹² However, in the present experiment, the loss of contrast allows one to estimate the momentum range. If the tip integrated over an infinite momentum range, the dI/dV maps would always exhibit atomic corrugations since SS₁ and SS₂ would provide a k state whatever the bias voltage. The loss of contrast rather suggests that the maximum momentum contributing to the tunneling current is smaller than $k_{\text{max}} = 0.6\bar{\Gamma}\bar{K} = 0.38 \text{ \AA}^{-1}$, as defined in Fig. 2(b). The onset of the SS₁ DOS at 1.05 eV corroborates this estimation. Indeed, a larger k_{max} would shift the onset to lower energy.

These surface states derive from the adatom sp_z dangling bonds, which are the elemental bricks of strongly correlated surfaces. Indeed, theoretical studies predict that the sp_z states weakly overlap on $\sqrt{3}$ surfaces, opening the way to strong correlation effects (large U/W ratio).¹⁻³ In the following,

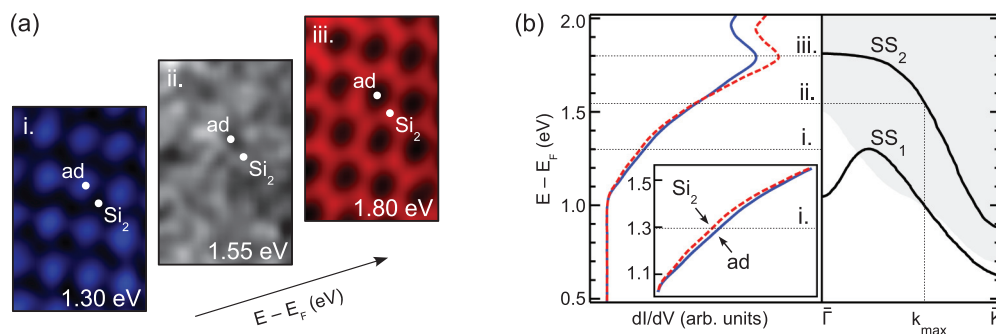


FIG. 2. (Color online) (a) dI/dV maps of the defect-free Si(111):B- $\sqrt{3}$ surface at (i) 1.30 eV, (ii) 1.55 eV and (iii) 1.80 eV bias voltages. (b) STS spectra recorded above a Si adatom (ad, solid blue line) and a second-layer Si atom (Si₂, dashed red line). The inset evidences the DOS difference in the low-energy sector. On the right, band dispersion of surface states SS₁ and SS₂ along $\bar{\Gamma}\bar{K}$ is shown; the shaded area represents the bulk continuum (from Ref. 11).

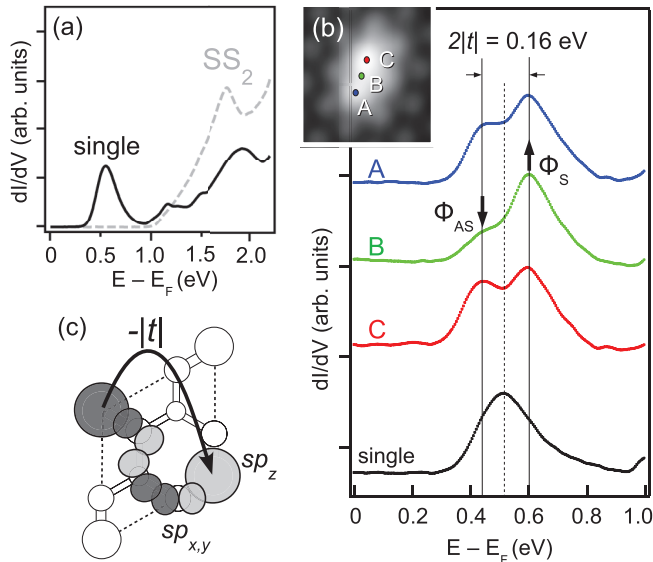


FIG. 3. (Color online) (a) Comparison of STS spectra recorded above a passivated adatom (dashed gray line) and a B vacancy (solid black line) ($U = 1.8$ V, $I = 0.4$ nA, $T = 5$ K). (b) Comparison of STS spectra recorded at different locations (A, B, and C) above a bivacancy and a single vacancy ($U = 2.0$ V, $I = 0.3$ nA, $T = 77$ K). (c) Schematics illustrating the indirect hopping path between nearest-neighbor adatoms. The dark and light gray lobes depict the positive and negative parts of the wave functions, respectively.

we propose a method to estimate the hopping parameter and, in turn, the strength of many-body interactions affecting dangling-bond surface states. We show that this information can be provided by local spectroscopy on impurities, namely, B (bi)vacancies. In Fig. 3(a), STS spectra recorded above a passivated adatom (dashed gray line) and a B vacancy (solid black line) are compared ($T = 77$ K). At the impurity site, an intense resonance appears in the intrinsic gap, as first pointed out by Berthe *et al.*⁸ This in-gap state results mainly from the localization of the SS_2 surface state, as demonstrated by the dramatic DOS transfer. The point is further supported by DFT calculations¹¹ that show that the SS_2 Wannier function has a significant B contribution, while the latter is negligible in the case of SS_1 .

With STS, it is possible to extract the Hubbard repulsion energy U of the impurity state. Recently, Nguyen *et al.* employed very high tunneling currents in order to reach a permanent regime corresponding to a singly occupied impurity.¹⁰ They observed a new spectral feature at higher energy, reflecting the charging of the impurity with a second electron. Their analysis yields $U = 1.12$ eV, in agreement with previous estimations.² Electrons occupying dangling bonds are affected not only by Coulomb repulsion but also by the coupling with local vibrations. The in-gap state, in principle decoupled from the other states, exhibits a surprisingly large linewidth (approximately 0.2 eV). Berthe *et al.* interpreted this feature within the Franck-Condon picture, the transport through the defect being dominated by a strong electron-vibration coupling and the formation of a local polaron.⁸ From a quantitative point of view, these authors extracted both the

vibration energy $\hbar\omega_0 = 32.5$ meV and the nondimensional coupling constant $g^2 = 9.6$.

In order to estimate the strength of many-body interactions and the possibility of a broken-symmetry ground state, the knowledge of the above parameters is not sufficient. The latter inform on the energy gained by electron localization. However, this effect competes with electron delocalization, whose energy scale is given by the hopping amplitudes. The analysis of the bivacancy defect allows us to extract this missing key parameter. In Fig. 3(b), we show STS spectra recorded at three different locations (A, B, and C; see inset) above the bivacancy defect. All spectra exhibit two resonances separated by 160 meV and shifted by ± 80 meV with respect to the single vacancy energy. This behavior is interpreted by analogy to the homonuclear diatomic molecule case. In such molecules, electron hopping lifts the atomic states degeneracy, with the formation of bonding and antibonding states. Their energy separation is $2|t|$, where t is the hopping integral; in the bivacancy case, we readily obtain $|t| = 80$ meV. Such a textbook problem was already realized, for example, in atomic chains built up by atomic manipulation.^{13,14}

While the spectra look very similar over the two adatom sites (A and C), the spectrum recorded in between (site B) shows a different shape, with a clear modification of the relative peak intensities. Indeed, the low-energy feature Φ_{AS} is weakened, while the high energy one Φ_S is strengthened. Due to inversion symmetry, the molecule eigenstates must be either symmetric or antisymmetric with respect to the center. As a general property, symmetric states show a maximum density between the atoms, whereas antisymmetric states exhibit a node at that same location. In the bivacancy, the analysis of the relative DOS at the center allows one to assign the symmetric state to the higher-energy state Φ_S and vice versa. This is at odds with the H_2 molecule case, where positive hopping between s orbitals ensures that the lowest-energy state is symmetric. Here, due to the large interadatom spacing (6.65 Å), the hopping between dangling bonds can only be *indirect*, hence the important role of the substrate in the hopping mechanism.¹⁵ An odd number of Si atoms in the sublayer is involved, resulting in a negative hopping. The situation is depicted in Fig. 3(c), where the indirect path between two nearest-neighbor sp_z orbitals involves bonds with p_x - p_y orbitals of three sublayer Si atoms.² Maximum bonding energy is achieved in the depicted configuration, with dangling bonds of opposite signs.

From the bivacancy hopping integral, we can, in turn, estimate the experimental SS_2 bandwidth. Indeed, both impurity and Bloch states derive from similar Wannier functions. On the hexagonal lattice, we get $W = 8|t| = 0.64$ eV, which compares fairly well with the bandwidth predicted by DFT¹¹ and measured by inverse photoemission.¹⁶ We are now able to estimate the strength of many-body interactions. Regarding electron correlations, a U/W ratio of 1.75 is found. This value fulfills the $U/W > 1$ condition for the Mott-Hubbard transition.¹ Polaronic effects lead to a renormalized Hubbard term $U_{\text{eff}} = U - 2g^2\hbar\omega_0$.¹⁷ In our case, $U_{\text{eff}} = 0.50$ eV. Therefore the interaction between polarons remains repulsive, so no bipolaronic ground state is expected to form. This finding supports the recent proposition that, contrary to a previous claim,^{18,19} K/Si(111):B has no bipolaronic ground state.²⁰

IV. CONCLUSION

In summary, we investigated the local electronic structure of the Si(111):B- $\sqrt{3}$ surface, a model system in the context of strongly correlated surfaces. We determined the strength of many-body effects affecting the dangling-bond surface states. Our finding strongly supports the realization of the Mott

insulator state on prototypical $\sqrt{3}$ -reconstructed surfaces. In order to tackle this problem, we developed a STS approach for bandwidth determination that relies on semiconductor impurities. This approach can be generalized to other semiconductor surfaces, where the usual standing-wave method²¹ is not applicable because of strong atomic corrugations.

*Present address: Institute of Condensed Matter Physics, Ecole Polytechnique Fédérale de Lausanne, CH-1015 Lausanne, Switzerland; cedric.tournier@epfl.ch

¹W. A. Harrison, *Phys. Rev. B* **31**, 2121 (1985).

²G. Santoro, S. Scandolo, and E. Tosatti, *Phys. Rev. B* **59**, 1891 (1999).

³E. Tosatti and P. Anderson, *J. Appl. Phys.* **2**, 2381 (1974).

⁴V. Ramachandran and R. M. Feenstra, *Phys. Rev. Lett.* **82**, 1000 (1999).

⁵R. Cortés, A. Tejada, J. Lobo, C. Didiot, B. Kierren, D. Malterre, E. G. Michel, and A. Mascaraque, *Phys. Rev. Lett.* **96**, 126103 (2006).

⁶S. Modesti, L. Petaccia, G. Ceballos, I. Vobornik, G. Panaccione, G. Rossi, L. Ottaviano, R. Larciprete, S. Lizzit, and A. Goldoni, *Phys. Rev. Lett.* **98**, 126401 (2007).

⁷G. Profeta and E. Tosatti, *Phys. Rev. Lett.* **98**, 086401 (2007).

⁸M. Berthe *et al.*, *Phys. Rev. Lett.* **97**, 206801 (2006).

⁹M. Berthe, R. Stiuflu, B. Grandidier, D. Deresmes, C. Delerue, and D. Stiévenard, *Science* **319**, 436 (2008).

¹⁰T. Nguyen, G. Mahieu, M. Berthe, B. Grandidier, C. Delerue, D. Stiévenard, and Ph. Ebert, *Phys. Rev. Lett.* **105**, 226404 (2010).

¹¹H. Q. Shi, M. W. Radny, and P. V. Smith, *Phys. Rev. B* **66**, 085329 (2002).

¹²C. Didiot, V. Cherkez, B. Kierren, Y. Fagot-Revurat, and D. Malterre, *Phys. Rev. B* **81**, 075421 (2010).

¹³N. Nilius, T. Wallis, and W. Ho, *Science* **297**, 1853 (2002).

¹⁴S. Fölsch, P. Hyldgaard, R. Koch, and K. H. Ploog, *Phys. Rev. Lett.* **92**, 056803 (2004).

¹⁵N. Nilius, T. M. Wallis, M. Persson, and W. Ho, *Phys. Rev. Lett.* **90**, 196103 (2003).

¹⁶T. Grehk, P. Mårtensson, and J. M. Nicholls, *Phys. Rev. B* **46**, 2357 (1992).

¹⁷R. Bari, *Phys. Rev. B* **3**, 2662 (1971).

¹⁸L. Cardenas, Y. Fagot-Revurat, L. Moreau, B. Kierren, and D. Malterre, *Phys. Rev. Lett.* **103**, 046804 (2009).

¹⁹C. Tournier-Colletta, L. Cardenas, Y. Fagot-Revurat, B. Kierren, A. Tejada, D. Malterre, P. Le Fèvre, F. Bertran, and A. Taleb-Ibrahimi, *Phys. Rev. B* **82**, 165429 (2010).

²⁰L. Chaput *et al.*, *Phys. Rev. Lett.* **107**, 187603 (2011).

²¹O. Jeandupeux, L. Bürgi, A. Hirstein, H. Brune, and K. Kern, *Phys. Rev. B* **59**, 15926 (1999).